Research Square

Preprints are preliminary reports that have not undergone peer review.
They should not be considered conclusive, used to inform clinical practice,
or referenced by the media as validated information.

Stage recycling of solar panels by pyrolysis and vacuum-free electric arc conversion to produce SiC

Kirill Larionov

laryk070@gmail.com

National Research Tomsk Polytechnic University

Roman Gerasimov

National Research Tomsk Polytechnic University

Zhanar Bolatova

National Research Tomsk Polytechnic University

Artur Gubin

Sevastopol State University

Vladimir Gubin

Sevastopol State University

Alexander Gorshkov

National Research Tomsk Polytechnic University

Alexander Pak

National Research Tomsk Polytechnic University

Anton Lavrenchuk

Sevastopol State University

Research Article

Keywords: solar panels, pyrolysis, vacuum-free electric arc conversion, silicon carbide

Posted Date: December 19th, 2025

DOI: https://doi.org/10.21203/rs.3.rs-8103737/v1

License: This work is licensed under a Creative Commons Attribution 4.0 International License.
Read Full License

Additional Declarations: No competing interests reported.

Version of Record: A version of this preprint was published at Silicon on September 11th, 2026. See the published version at https://doi.org/10.1007/s12633-026-03798-x.

Stage recycling of solar panels by pyrolysis and vacuum-free electric arc conversion to produce SiC

Kirill Larionov[1, 2*], Roman Gerasimov[1], Zhanar Bolatova[1], Artur Gubin[3], Vladimir Gubin[1,3],
Alexander Gorshkov[1], Alexander Pak[1] , Anton Lavrenchuk [3]
[1]National Research Tomsk Polytechnic University, Tomsk, 634050, Russia
[2]Gorbachev Kuzbass State Technical University, Kemerovo, 650000, Russia
[3]Sevastopol State University, Sevastopol, 100000, Russia
*Corresponding author
E-mail address: laryk070@gmail.com
ORCID ID: 0000-0003-0340-9461

Abstract

The rapid growth in the number of solar panels worldwide is making the issue of their utilization increasingly urgent. This paper presents a combined approach to recycling spent solar panels. The polymeric components were processed by pyrolysis to produce carbon residue and synthesis gas, while the inorganic components underwent plasma treatment to produce silicon carbide (SiC). Pyrolysis at 500 °C produced synthesis gas containing up to 5 vol.% methane, as well as carbon monoxide (CO) and carbon dioxide (CO_2), with maximum concentrations of up to 0.6 vol.%. The average yield of carbon residue was 45.8 wt.%. Vacuum-free electric arc treatment ensured the synthesis of silicon carbide. According to X-ray phase analysis, increasing the carbon content of the mixture from 0% to 30% resulted in an increase in the SiC fraction from 46% to 61%, while the fractions of free silicon and silicon oxide decreased simultaneously. This approach not only ensures efficient management of solar panel waste but also enables the recovery of useful resources for further utilization.

Keywords: solar panels, pyrolysis, vacuum-free electric arc conversion, silicon carbide

1. Introduction

Rapid population growth and industrial development have led to a significant increase in pollution worldwide. One way to mitigate this negative environmental impact and meet the growing demand for energy is to replace non-renewable energy sources, such as fossil fuels, with clean, renewable alternatives [1]. Solar energy is one of the key renewable sources that could account for a large proportion of energy generation. It is safe, does not pollute the environment, and does not harm ecosystems. Furthermore, solar energy is reliable, affordable, efficient, and can be utilized on a large scale [2].

One method of converting solar energy into electricity involves using solar panels with photovoltaic cells. These cells generate a flow of electrons when exposed to sunlight. The electrons then move through a closed circuit, creating a direct current that can be used to power devices or stored in batteries. Solar panels are also known as photovoltaic modules or solar electric panels.

Although solar panels are environmentally friendly, they can become a source of hazardous waste once they reach the end of their 20- to 30-year lifespan [3]. With an increasing number of failed solar systems and a lack of knowledge about proper disposal, photovoltaic (PV) system waste is becoming a serious global issue. As many developed countries have been installing PV systems since the 2000s, a significant increase in this type of waste is expected by 2030. Currently, a large proportion of the original installations are reaching the end of their useful life. This creates a pressing need for the efficient management of PV systems that can no longer be used. The International

Renewable Energy Agency predicts that PV waste will reach between 1.7 and 8 million tonnes by 2030 and between 60 and 78 million tonnes by 2050 [4, 5].

To date, three main types of solar cells have been widely used: Crystalline silicon (Si) cells (comprising 40% monocrystalline, 48% polycrystalline, and 2% ribbon silicon); thin-film cells (including 5% cadmium telluride (CdTe), 2% amorphous silicon (a-Si), and 2% copper indium gallium selenide (CIGS)); and concentrating solar cells and emerging technologies (accounting for 1%, including dye-sensitized solar cells, organic solar cells, and hybrid cells) [6]. The primary recycled components of photovoltaic (PV) panels are glass (approximately 68 wt.%), aluminum (approximately 15 wt.%), high-purity silicon (approximately 3 wt.%), and copper cables (approximately 1 wt.%) [7].

The production of silicon, the main component of solar panels, incurs high energy costs. In addition, solar panels contain heavy metals such as lead, cadmium, and tin, which can pollute the environment and pose a threat to human health if not disposed of properly. Therefore, it is essential that the components of solar PV panels are collected and disposed of in a responsible manner.

There are currently various approaches to recycling solar panels and their components, including chemical, physical, thermal, and combined methods. Authors [8, 9] distinguish three technological methods for solar panel recycling: upcycling (high-value recycling), recycling (medium-value recycling), and downcycling (low-value recycling). In downcycling, PV module waste is processed through mechanical methods such as crushing, sieving, and metal separation to separate the materials within the modules. This process results in broken glass that can be used in the production of foam or glass fiber. The recovered metals can be reused through melting and recycling. Any remaining waste is typically incinerated or composted in smaller quantities. This recycling approach minimizes landfill waste and incurs relatively low energy and processing costs. However, it is important to note that the quality of the recovered materials can vary, which limits their recyclability [10, 11].

In the 'recycling' technology, the aluminum frame, outer glass, and junction box are mechanically removed from crystalline silicon-based photovoltaic (PV) modules. The remaining waste is then shredded and mixed with polypropylene and low-density polyethylene to produce pressed tiles [10]. While this method is inexpensive and straightforward, it does not always offer cost-effective recycling and may fail to meet the required recycling volumes for this type of waste.

On the other hand, the 'upcycling' technology involves the delamination of the module using various methods, such as thermal [12, 13], mechanical [14, 15], and chemical [16, 17] delamination, followed by the extraction of glass, silicon wafers, and valuable metals. However, mechanical fragmentation does not always result in complete separation of the PV modules and requires subsequent thermal (e.g., pyrolysis) or chemical treatment, depending on the composition of the different fractions [18]. Chemical stratification is a more costly method, but it allows for separation at low temperatures while maintaining the integrity of the solar panel. Nevertheless, this method has the disadvantage of involving toxic reagents, the vapors of which can be harmful to human health.

Thermal recycling methods (module delamination) involve altering the properties of solar panels and decomposing polymer materials at high temperatures. This process enables the mechanical separation of pure glass from the silicon components. The pyrolysis method is most commonly used to remove polymers from silicon and metal components in solar panels [13, 19, 20].

Wang and Xiao [19] proposed a thermal method for recovering silicon, glass, and metals from crystalline silicon (c-Si)-based modules. This process consists of two heating steps. First, the backsheet of the solar panel is separated at 330 °C for 30 minutes. In the second step, the EVA polymer is scorched at 400 °C for 120 minutes. This two-step process yields a glass plate that can be used in new modules at a controlled temperature.

The temperature regime in the reactor and the duration for which the sample remains in the medium are critical factors in thermal conversion processes. For instance, the authors of [20] conducted pyrolysis on a photovoltaic (PV) cell sample at 500 °C for 30 minutes. They found that this treatment method removed more than 99% of the polymers present in PV modules. In another study [13], direct pyrolysis of PV modules in a nitrogen atmosphere resulted in an 80% glass recovery under optimum operating conditions.

Plasma technology plays a crucial role in the recycling and reuse of materials from waste solar panels. Plasma arc technology generates extremely high temperatures that break molecular bonds in materials, facilitating the separation of various components, including metals, semiconductors, and polymers. The high-temperature plasma environment also promotes chemical transformations that can convert waste materials into valuable resources for various industries. For example, silicon carbide (SiC) is highly sought after in the market due to its exceptional properties, such as high hardness, thermal conductivity, and corrosion resistance. This not only brings economic benefits but also helps reduce negative environmental impacts while conserving valuable resources [21, 22].

In [23], silicon carbide (SiC) was synthesized from spent solar panels containing 35% silicon and compact discs containing 20% carbon, using a thermal plasma arc. X-ray diffraction (XRD) and X-ray photoelectron spectroscopy (XPS) analyses confirmed the formation of silicon carbide (SiC) and silicon (Si) phases.

An important aspect of developing plasma methods for utilizing waste is simplifying the design and enhancing energy efficiency by eliminating the need for vacuum equipment, generators, or cylinders containing inert gases. One solution to improve the efficiency of plasma technologies is the application of the vacuum-free electric arc conversion method, which can be used to process silicon-containing waste [24, 25] and produce silicon carbide. This method involves reaching the temperature required for the carbothermal reduction of oxide phases through the thermal field generated by the arc discharge. Due to the formation of CO and CO_2 gases in the reaction zone at the initiation of the arc discharge in an open-air environment, the working volume of the reactor is shielded from oxygen. Consequently, reduction processes can occur with the formation of carbides when the conditions for self-shielding of the reaction volume are met. Therefore, identifying effective methods for collecting and recycling solar panel components remains an urgent task.

This paper presents the results of an experimental study on the recycling of spent solar panels using pyrolysis and vacuum-free plasma electric arc conversion methods, with the aim of obtaining carbon residue, silicon carbide, and synthesis gas that can be used for energy production.

2. Materials and methods

A typical polycrystalline silicon solar panel, which had been used and was no longer fit for purpose, was obtained from one of the enterprises in the fuel and energy complex in the Republic of Crimea (Russia). This panel was used as the sample for the investigation.

The morphology and elemental composition of the sample were examined using scanning electron microscopy (SEM, Tescan Vega SBU3, Czech Republic) with an energy-dispersive X-ray spectroscopy (EDS) attachment. Fig. 1 shows the different fractions of the spent solar panel that were recycled by pyrolysis and placed on a carbon substrate.

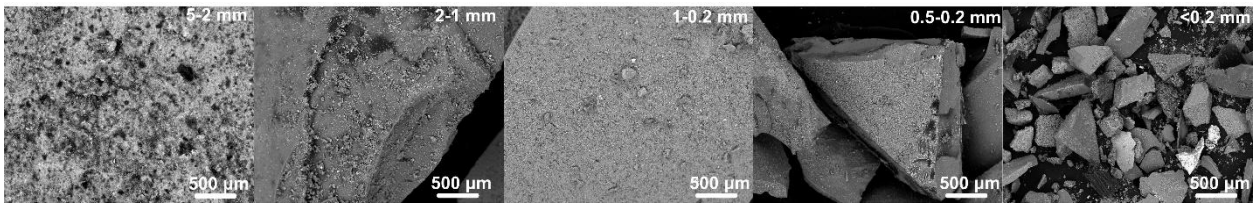


Fig. 1 SEM images of solar panels of different fractions after pyrolysis treatment

The scanning electron microscopy (SEM) results show that the samples with fraction sizes of 5–2 mm and 2–1 mm consist of irregularly shaped particles, with a maximum size distribution of several tens of micrometers. According to the energy-dispersive X-ray spectroscopy (EDS) data (Table 1), the recycled solar panels primarily consist of silicon, along with several impurities. The main impurities are aluminum and titanium (up to 11% by weight), with smaller quantities of tin (up to 2% by weight) also present. The EDS data indicate that silicon is the dominant element in all samples on average. The EDS results for the solar panels are consistent with existing data on the chemical composition of spent solar panels [26, 27].

The 1–0.5 mm sample exhibits particle morphology characterized by lumpy irregularities, representing loosely textured micron-sized particles measuring less than 10 μm. The 0.5–0.2 mm fractions are characterized by particles arranged on their surfaces. These particles are presumably composed of silver and may be associated with the silicon charge; their size does not exceed 100 μm.

Table 1 Particle distribution and elemental composition of spent solar panels following thermal recycling by pyrolysis, for fractions of less than 0.2 mm

Fraction	Weight,g	Weight fraction, %	Elemental content, %								
			Si	Al	Ag	Ti	Fe	Sb	Pb	Sn	Cu
After pyrolysis	-	-	61,23	21,01	5,14	4,42	2,52	1,90	1,06	0,85	1,87
5–2 mm	1,99	21,17	60,9	22	4,99	4,15	2.10	1.76	1,40	0,70	-
2–1 mm	2,84	30,28	60,42	10,65	3,47	8,17	0,27	2,89	4,55	5,55	2,81
1–0,5 mm	2,73	29,12	58,5	21,88	6,04	9,15	0,13	0,81	1,52	1,29	-
0,5–0,2 mm	1,48	15,77	56,14	13,3	5,69	17,59	0,25	1,12	2,56	2,57	-
< 0,2 mm	0,34	3,66	44,39	13,75	12,82	15,05	0,7	0,86	6,88	4,74	-

The pore size in the 0.5–0.2 mm sample (Fig. 2) is less than 100 μm and consists of conglomerates of many small, irregularly shaped porous particles. The porous texture is clearly visible on the surface, indicating the material's complex structure and its interaction with the environment.

Samples with a particle size of less than 0.2 mm, as shown in Fig. 2, consist of particles smaller than 200 μm, among which large silicon particles are prominent. On the contact surface of these particles, agglomerated, dispersed aluminum oxide particles are observed, with sizes ranging from 10 to 40 nm. These particles are regular in shape and possess a cubic crystal lattice.

A cluster of particles, which could presumably be silver or lead, is also observed on the surface of the aluminum oxide. The high silicon-to-aluminum (Si/Al) ratio indicates the presence of zeolites and sodalites in the sample's composition.

Thus, the analysis demonstrates the diversity of the morphological characteristics and constituent components of the recycled fractions of spent solar panels.

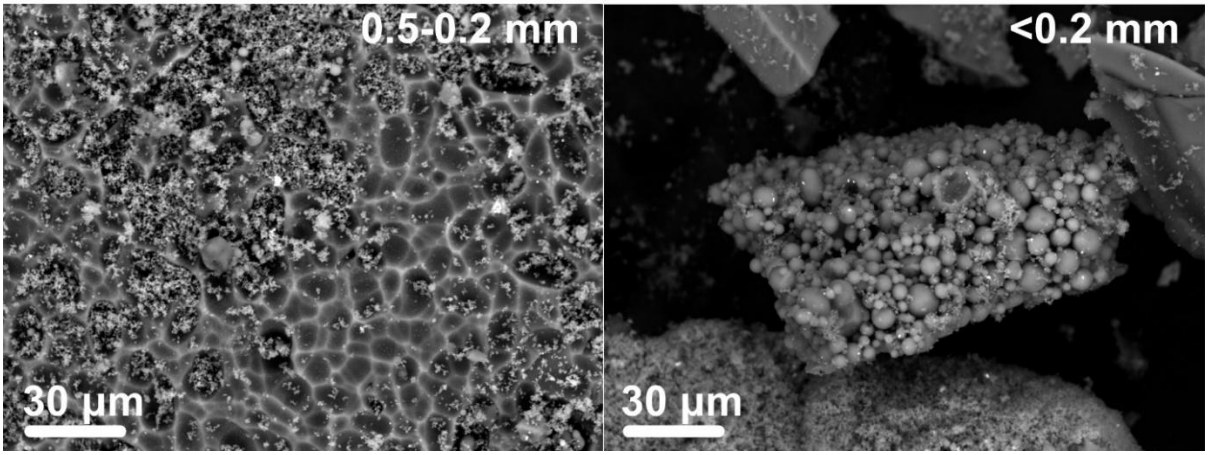


Fig. 2 SEM images of solar panel particles with a fraction of 0.5 mm and less than 0.2 mm after their pyrolysis treatment

2.2 Pyrolysis

A thermal analysis was performed using a STA 449 C Jupiter thermal analyzer (Netzsch, Germany) to determine the required temperature for the pyrolysis process of the crushed sample of spent solar panels. The analysis was conducted in an argon atmosphere with a flow rate of 150 mL/min, at a heating rate of 10 °C/min, up to 1000 °C. The mass of the sample loaded into the corundum crucible was approximately 10 mg. The decomposition characteristics, including the initial and final decomposition temperatures (T_d and T_f, respectively), the maximum decomposition rate (w_{max}) at the characteristic temperature (T_{max}), were evaluated using thermogravimetric (TG) and differential thermogravimetric (DTG) data.

The pyrolysis process was investigated using a laboratory setup, the schematic diagram of which is shown in Fig. 3.

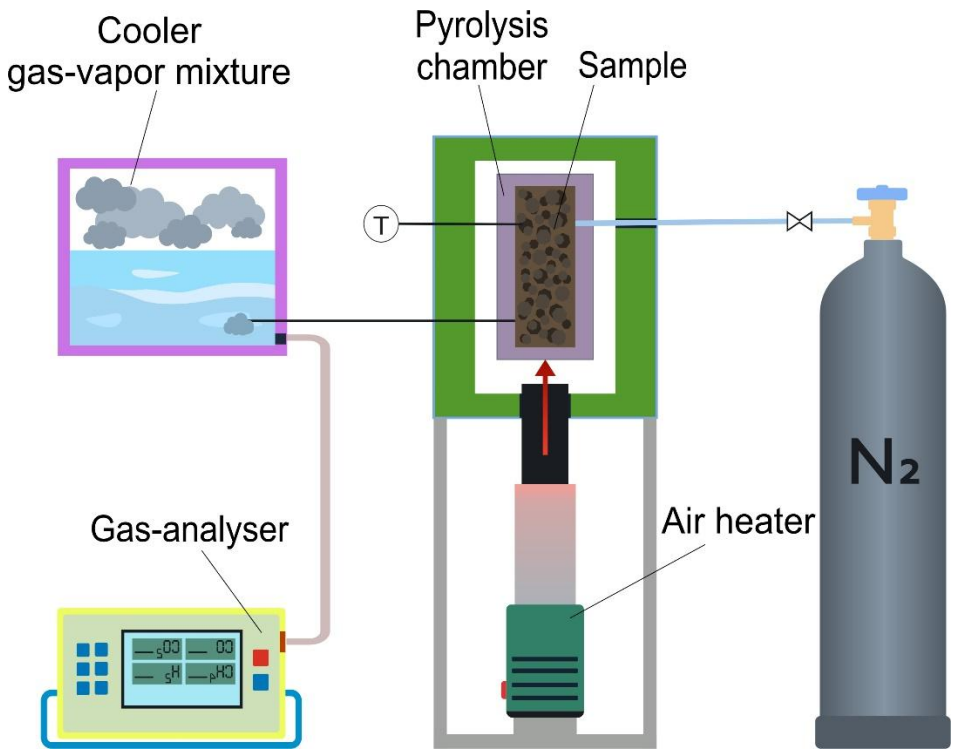


Fig. 3 Schematic diagram of a laboratory unit for pyrolysis of hydrocarbon materials

A fractionated sample of spent solar panels was placed in a cylindrical reactor with a volume of 145 mL (height: 115 mm; diameter: 40 mm), which was operated in batch mode. Depending on the bulk density of the samples, about 70–80% of the reactor volume was filled. Heat was supplied indirectly to the bottom of the reactor by preheating the air using an LHS 61L PREMIUM temperature-controlled air heater (Leister Technologies AG, Kaegiswil, Switzerland), which provides a high airflow rate and a maximum heat output of 16 kW at a maximum heating temperature of 650 °C. An AIRPACK high-pressure fan (Leister, Kaegiswil, Switzerland) supplied air to the heater. The coolant temperature reached 500 °C. The temperature inside the reactor was continuously monitored using a thermocouple (type T) connected to an electronic recorder (Thermodat-25E6, Thermodat, Perm, Russia). During the pyrolysis process, the reactor chamber was purged continuously with nitrogen at a flow rate of 2 L/min.

The vapour gases generated during the pyrolysis process were cooled by bubbling them through water in a 100 mL vessel (height: 80 mm; diameter: 40 mm), which contained 60 mL of water. The non-condensable gas-phase products of pyrolysis were analyzed using a Test-203 in-line gas analyzer (BONER, Novosibirsk, Russia). The concentration measurement ranges of the gas analyzer were: O_2: 0–21 vol.%, CO: 0–50 vol.%, CO_2: 0–100 vol.%, H_2: 0–40 vol.%, and CH_4: 0–50 vol.%. The relative error of the measurements was ±5%. Measurements were taken periodically at 3-second intervals.

In the first stage of the experimental study, the reactor and a sample of spent solar panels were indirectly heated to a target temperature (Tg = 500 °C). The heating rate was 60 °C/min, which is typical for a slow pyrolysis process [28, 29]. Once the target temperature (T_g) was reached, the reactor was maintained at a constant temperature until the pyrolysis process was complete. Pyrolysis was considered complete when no gas-phase compounds (CO, CO_2, CH_4, and H_2) were present, as determined by an in-line gas analyzer. The reactor was then cooled. The heating and cooling rates of the reactor were controlled by varying the AC frequency of the air blower.

2.3 Vacuum-free electric arc conversion

Vacuum-free electric arc conversion was carried out using a specialized laboratory setup. The key component of the setup is a DC reactor with a vertically arranged set of electrodes. A schematic diagram of the setup is shown in Fig. 4. The laboratory unit includes a power supply, an electrode positioning system, a cooling system, a conversion products removal system, a system for recording the arc's electrical parameters, and an in-line gas analyzer (Test-1, Boner, Russia). A notable feature of the unit is that an inert gas atmosphere is not required due to the formation of a self-protective atmosphere in the arc combustion zone [30].

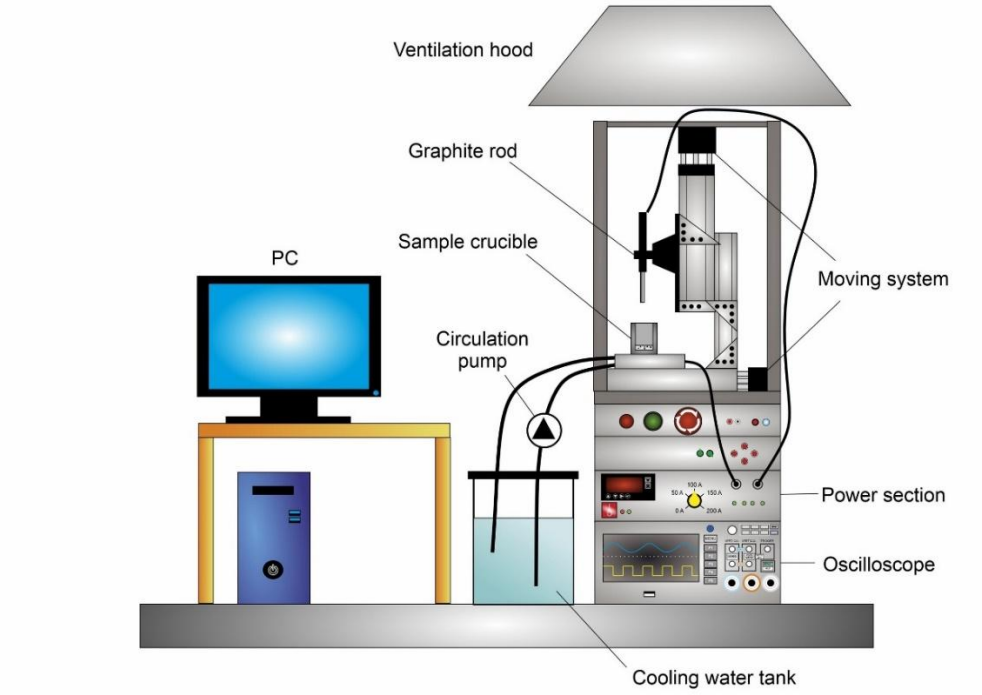


Fig. 4 Schematic diagram of a laboratory setup for vacuum-free electric arc conversion

The reactor zone consists of a graphite crucible with a height of 40 mm, an outer diameter of 30 mm, and a wall thickness of 5 mm. A mixture of initial reagents, weighing approximately 2 g, is loaded into the crucible. An anode, in the form of a graphite rod, is used, with a diameter of 10 mm and a length of 130 mm. The bottom of the crucible serves as the cathode. To ensure precise positioning of the anode relative to the cathode, an automated handling system is employed. The arc discharge is initiated by bringing the electrodes closer together, after which the anode is withdrawn by 1–2 mm from the carbon felt graphite pad. This initiates the process of high-temperature synthesis, which occurs within the closed volume of the crucible's inner cavity.

The unit is operated via specialized software, which allows for the configuration of parameters such as current strength and arc duration. During the experiment, current and voltage are monitored using a Rigol DS1052E digital oscilloscope to assess the stability of the arc and the energy characteristics of the process. A ventilation system prevents the accumulation of gases and graphite combustion products. Once the fusion process is complete, an active heat sink system is activated to accelerate the cooling of the crucible.

For the initial charge, shredded solar panels with a particle size of approximately 1 mm were used, along with pre-pyrolyzed samples containing varying carbon content. Technical carbon grade N550 was also included in the

charge composition. The addition of carbon is necessary to provide conditions for the carbothermal reduction (SiO_2 → SiC) of silicon in the reaction zone, as per the known reactions:

$$SiO_2 + 3C \rightarrow SiC + 2CO \quad (1)$$

The selected synthesis conditions are as follows: synthesis time of 60 seconds and current strength of 200 amperes. These parameters are necessary to achieve temperatures exceeding 1800 °C, which are required for the silicon carbide synthesis reactions. Similar conditions were successfully tested in our previous studies [24], where the efficiency of atmospheric electric arc technology for processing silicon-containing waste was demonstrated.

An automated movement system is employed for the coaxial movement of the anode relative to the cathode. Once the electrodes make contact, the anode is moved to a distance of approximately 1–2 mm from the graphite felt pad, initiating the arc discharge. This setup maintains the arc discharge within the inner crucible cavity.

2.4 Characterisation of the electric arc conversion/synthesis product

The microstructure of the samples obtained from electric arc conversion/synthesis was analyzed using a JSM-6000C scanning electron microscope (JEOL, Japan), equipped with an autoemission cathode.

The crystalline phases were identified using X-ray diffractometry (XRD) with a Shimadzu XRD 7000S (CuKα, λ = 1.5406 Å) and standard diffractometer software, in conjunction with the PDF4+ structural database.

The oxidation process was investigated using a Netzsch STA 449 F3 Jupiter thermal analyzer (Netzsch, Germany). The analysis was carried out at a heating rate of 10 °C/min in a corundum crucible with a perforated lid, up to a temperature of 1000 °C. The sample, weighing approximately 10 mg, was evenly distributed in a layer on the bottom of the crucible and subjected to a flow of oxidizing air. The gas flow rate was 150 ml/min, and all experiments were conducted under atmospheric pressure conditions.

A comparative evaluation of the thermal conversion process parameters for samples in different media was performed based on physical quantities (temperature, time, and process rate), which were calculated graphically using TG and DTG profiles.

3. Results and discussions

3.1 Pyrolysis

The results of the thermal decomposition study of the solar panel sample in an inert argon environment are presented in Fig. 5.

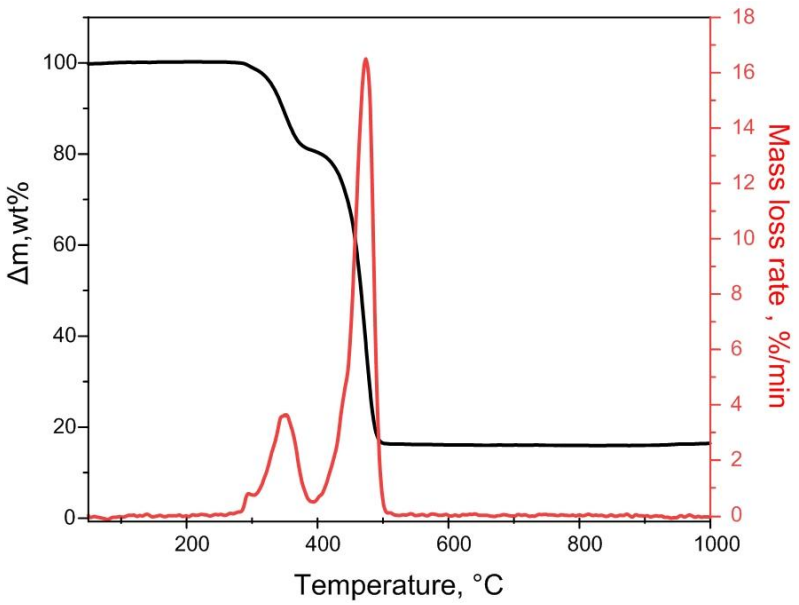


Fig. 5 TG and DTG data for inert decomposition of the solar panel. Heating rate 10 °C/min, argon flow rate 150 ml/min.

The thermal decomposition of solar panels in an inert environment is primarily driven by the polymer binder, ethylene-vinyl acetate (EVA). Solar panels exhibit thermal stability up to 282 °C. This process occurs in two stages: the first stage, from 282 to 377 °C, is characterized by the production of acetic acid [31, 32], while the second stage, from 377 to 498 °C, involves the decomposition of vinyl acetate. No thermal transformations are observed in the high-temperature region up to 1000 °C. The obtained results are consistent with those reported by other authors [31, 32].

The dependence of the concentration of gas-phase compounds (CO, CO_2, and CH_4) formed during pyrolysis on the laboratory bench is presented in Fig. 6.

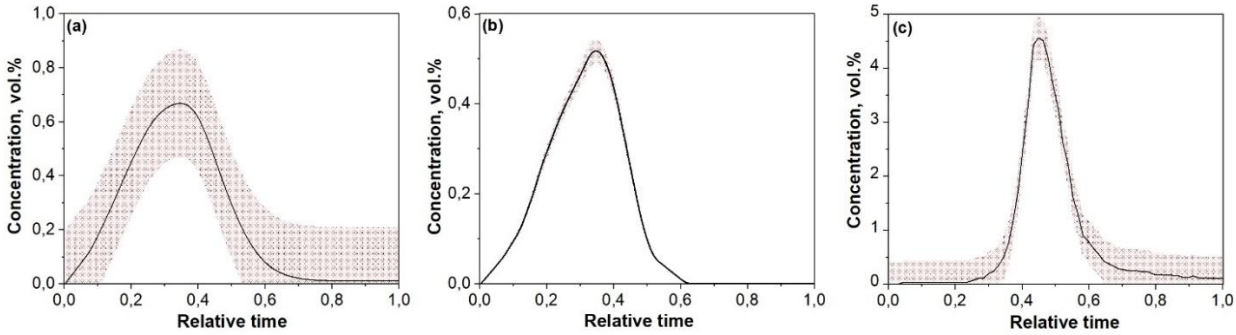


Fig. 6 Concentration dependences of the formation of gas-phase compounds during pyrolysis of a sample of spent solar panels - CO (a), CO_2 (b) and CH_4 (c)

Pyrolysis experiments were conducted repeatedly, and the non-condensable gaseous stream was characterized by an absence of oxygen and a low volume of the aforementioned products. This is due to the preferential formation of acetic acid and alkenes [33]. The peak concentrations of CO and CO_2 do not exceed 0.6 vol.%, while for CH_4, this value reaches 5 vol.%. The observed shift in peak timing can be attributed to the secondary decomposition of acetic acid, which forms CO and CO_2 at low temperatures, and the decomposition of methyl vinyl at higher temperatures.

The average yield of pyrolysis carbon residue was 45.8 wt%, which is significantly higher than the value of 36.8 wt% determined by STA. This discrepancy is due to the experimental setup; specifically, the larger volume of

raw materials used in the reaction zone results in different heat transfer conditions and an increased influence of secondary reactions leading to the formation of semicoke. These reactions are further enhanced by the presence of mineral components in the solar panels [34].

3.2 Vacuum-free electric arc conversion

Fig. 7 shows how the concentration of gas-phase compounds (O_2, CO, CO_2, H_2 and CH_4) produced during the vacuum-free plasma electric arc conversion conversion of the solar panel sample changes.

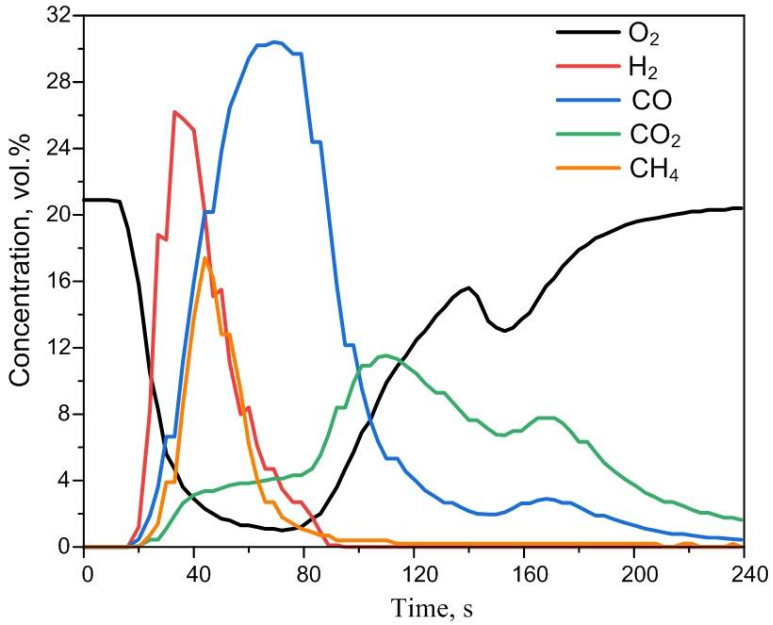


Fig. 7 Concentration dependences of gas-phase compound formation during plasma conversion of solar panel sample

The maximum concentrations during the vacuum-free electric arc conversion of the solar panel sample reached 30.4, 26.2, and 17.4 vol.% for CO, H_2, and CH_4, respectively. These curves exhibit a typical monomodal distribution, which is characteristic of similar processes [35]. The bimodal distribution of the curve representing CO_2 release can be attributed to the specific conditions of the experiment and the method used for registering the gas-phase products.

Fig. 8 shows the results of X-ray diffraction (XRD) analysis of powders obtained by electric arc conversion of different samples of spent and pyrolyzed solar panels, as well as a sample without pretreatment by pyrolysis.

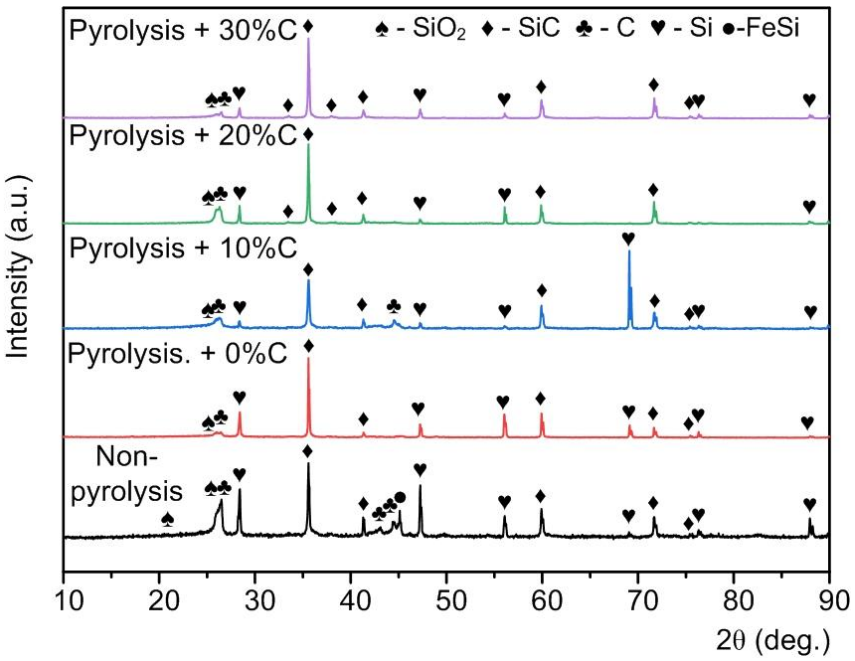


Fig. 8 Diffractograms of samples with and without pyrolysis pretreatment obtained by exposure to a vacuum-free electric arc reactor

Based on the analysis of the diffractograms, it can be concluded that the main peak in the initial solar panel sample, without preliminary pyrolysis treatment, corresponds to the cubic phase of silicon carbide (No. 65-360). Additionally, phases of silicon oxide (No. 89-8938), silicon (No. 01-075-0589), and hexagonal graphite (No. 89-8487) are also present. At 45°, peaks corresponding to the hexagonal phase of iron silicide (No. 86-793) are observed. The formation of iron silicide is further corroborated by the elemental analysis results, which identified iron in the solar panel fractions [36]. Several studies have also confirmed the formation of silicon carbide phases during the plasma processing of solar panels. For instance, in [26], silicon carbide with a rhombohedral structure was obtained during processing.

A series of chemical reactions occur during the arc discharge combustion, which can be described by the following equations:

$$SiO_2 + 3C \rightarrow SiC + 2CO;$$

$$C + O_2 \rightarrow 2CO;$$

$$CO + O_2 \rightarrow 2CO_2$$

$$2Si + Fe \rightarrow FeSi_2$$

The samples subjected to pre-pyrolysis treatment exhibit the presence of hexagonal graphite phases, cubic silicon phases, and rhombohedral silicon carbide phases. Increasing the carbon content of the mixture from 0% to 30% results in a decrease in the proportion of silicon phases from 19.7% to 8.3%, and silicon oxide from 3% to trace amounts. In contrast, the silicon carbide content increases from 46% to 61%. The lattice parameters of cubic silicon carbide are a = 3.08060 Å ± 0.0002 Å.

It is also noteworthy that the peak corresponding to the iron silicide phase disappears during the pyrolysis pre-treatment of the solar panels. This suggests that the pyrolysis process may partially convert iron to iron oxide [37], particularly in the presence of oxygen. The resulting iron oxide may either become incorporated into the solid carbon residue or, depending on the pyrolysis conditions, escape as a gas. Consequently, during subsequent plasma treatment, silicon carbide (SiC) is predominantly formed, with minimal iron silicide impurities.

Faint traces of quartz observed in the samples could be attributed to the initial powders not being adequately processed during electric arc exposure or to the silicon carbide undergoing surface oxidation during the cleaning process. The presence of graphite is likely due to residue in the particle agglomerates resulting from incomplete combustion. However, because the sample is a mechanical mixture with varying particle sizes, a complete transition of components has not been achieved. To improve the homogeneity of the composition, additional homogenisation of the charge or repeated arc treatment is recommended [24].

Fig. 9 shows the diffractograms for the samples before and after repeated exposure to arc discharge without the addition of carbon. The proportion of silicon carbide decreased by 11%, while the proportion of silicon oxide increased by 2%. The silicon carbide produced exhibits an inhomogeneous morphology. This increase in silicon oxide and the appearance of additional silicon oxide maxima, along with the decrease in silicon carbide, is likely due to the passive oxidation of silicon carbide. This oxidation process can be described by the following reactions [38, 39]:

$$2SiC + 3O_2 \rightarrow 2SiO_2 + 2CO$$

As described in the paper [40], silicon formation can occur through the oxidation of the powder surface, with the reaction proceeding as follows:

$$SiC + O \rightarrow Si + CO.$$

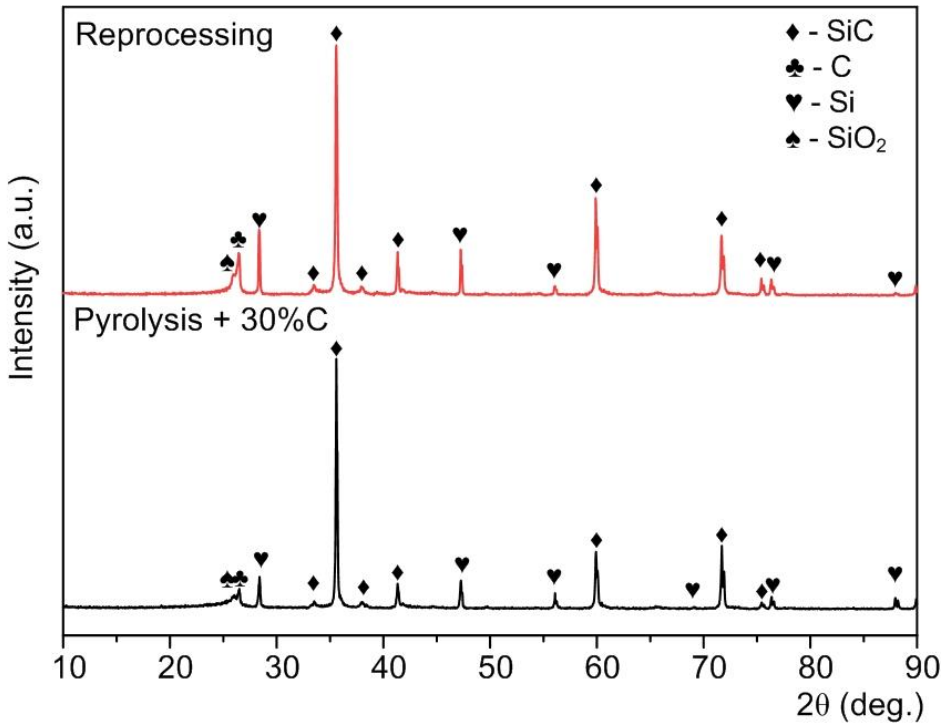


Fig. 9 Diffractograms of the tested samples before and after pretreatment of the samples in a vacuum-free electric arc reactor

Thermogravimetric analysis in air was performed to evaluate the mass ratio for samples after arc exposure without and with pyrolysis pretreatment (Fig. 10).

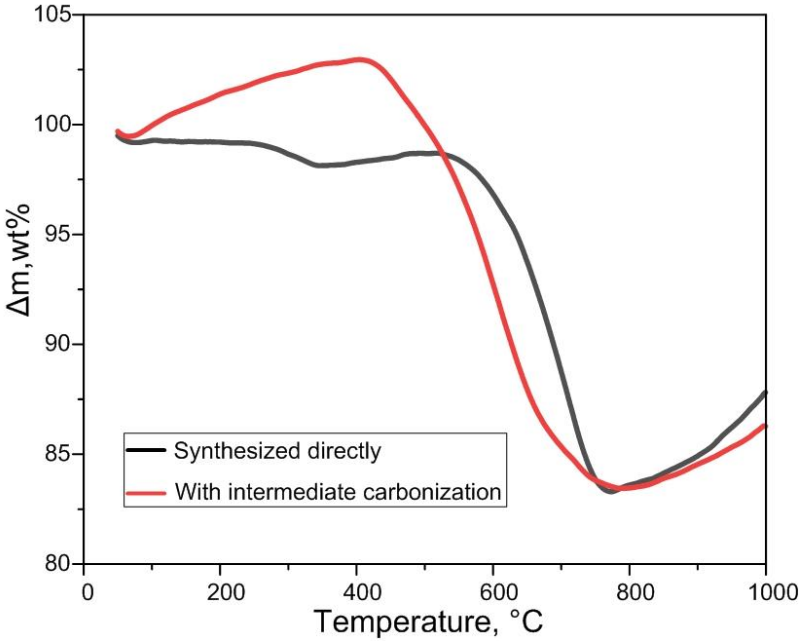


Fig. 10 TG data for the oxidation process of SiC: synthesized directly and with pretreatment by pyrolysis

According to the obtained data, the following main oxidation stages can be distinguished: mass loss in the temperature range of 600–750 °C, and mass gain from 750 °C onwards. The mass loss is associated with the oxidation of carbon that underwent high-temperature conversion but did not react with silicon. The mass gain is attributed to the oxidation of silicon carbide [41]. The presence of two components that did not fully interact during the relatively long processing period may be due to the configuration of the processed solar panels, which were represented by particles with characteristic sizes on the order of millimetres. The slight increase in mass, as shown in the graph on the right, may be due to the chemisorption of oxygen onto carbon.

Fig. 10 also shows scanning electron microscopy (SEM) micrographs of silicon carbide samples obtained from a thermally untreated solar panel and a pre-pyrolyzed sample.

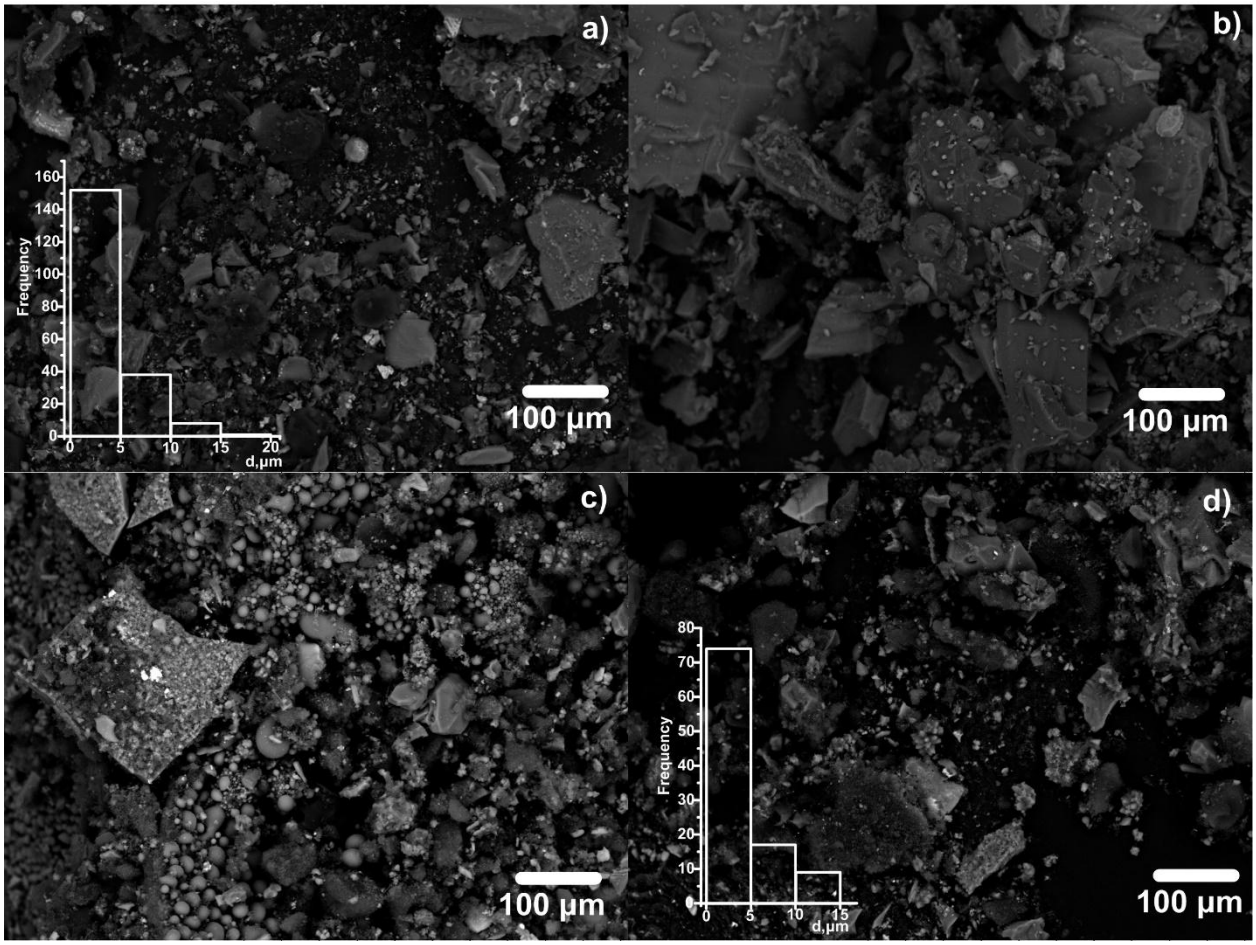


Fig. 11 SEM images of the obtained SiC: synthesised directly by arc exposure (a) and (b,c,d) synthesised by arc exposure with pyrolysis pretreatment

According to the results of scanning electron microscopy (SEM), a variety of particle morphologies are observed in the samples of spent solar panels exposed to the arc with and without pyrolysis pretreatment. Fig. 11a shows the samples without pyrolysis pretreatment: the particle size reaches 20 μm and above, with spherical-shaped particles observed. In the sample with intermediate carbonization, silicon carbide (SiC) particles with a regular hexagonal shape are distinguishable, although spherical silicon formations are also present. Fig. 11c clearly shows spheres up to 10 μm in diameter, which are most likely not silicon carbide, as SiC particles typically exhibit irregular shapes; these are likely to be metal or silicon oxides. Fig. 11d depicts the same powder but from a different region of the field of view. Fig. 11b shows irregularly shaped agglomerates, morphologically similar to silicon carbide; similar structures have been described in other works [26, 42].

In general, the particles exhibit a wide size range—from units to tens of micrometers—and diverse morphologies, including cubic, agglomerated, and irregular shapes. The results obtained emphasize the complexity of the morphology and composition of the products processed by vacuum-free electric arc conversion of solar panels, highlighting the need for further research in this field.

Conclusion

The studies confirmed the efficiency of the combined method for utilizing used solar panels. Pyrolysis at 500 °C facilitated the removal of polymer components and the production of synthesis gas containing up to 5 vol.% methane, as well as up to 0.6 vol.% CO and CO_2. The average yield of carbon residue was 45.8 wt.%. Vacuum-free

electric arc treatment of the inorganic fraction produced silicon carbide (SiC), which accounted for up to 61% of the solid residue by mass, with optimal carbon content in the charge. The remaining phases consisted primarily of free silicon and smaller amounts of silicon oxide. However, repeated electric arc synthesis of the products without additional carbon led to the oxidation of silicon carbide, increasing the proportion of silicon oxide by 2%, as confirmed by X-ray diffraction analysis.

Notably, the iron silicide phase was completely eliminated during the pyrolysis pretreatment, improving the purity of the final product and expanding its potential applications.

Thus, the integration of pyrolysis and vacuum-free electric arc conversion enables efficient recycling of waste solar panels and the production of valuable, high-added-value products. The recovery of silicon carbide from waste solar panels offers new opportunities for resource reuse across various industries, reduces environmental impact, and contributes to the development of a circular economy.

Future research may focus on optimizing the technological parameters of both processing stages to increase the yield of target products and reduce energy costs.

Funding: The study was supported by the Ministry of Science and Higher Education of the Russian Federation (project No. FSWW-2025-0003).

Declarations

Conflict of interest The authors declare that they have no competing financial interests.

References

1. Al, B.A., Maghraby, Y.R., Ibrahim, A.H., Shouier, K.R., Alturki, A.M., El-shabasy, R.M. Role of green chemistry in sustainable corrosion inhibition: a review on recent developments. Mater. Today Sustain. 2022; https://doi.org/10.1016/j.mtsust.2022.100242
2. Mulazzani, A., Eleftheriadis, P., Leva, S. Recycling c-Si PV modules: A review, a proposed energy model and a manufacturing comparison. Energies. 2022; https://doi.org/10.3390/en15228419
3. Maghraby, Y.R., Ibrahim, A.H., Tayel, A., Mohamed, H., Azzazy, E. Towards sustainability via recycling solar photovoltaic Panels , A review. Sol. Energy. 2025; https://doi.org/10.1016/j.solener.2024.113085
4. Cells LPS, Xing J, Hao L, Mashingaidze MM. A review of recent developments in preparation methods. Coatings. 2022; https://doi.org/10.3390/coatings12020252
5. Yu HF, Rahim NA, Amin N. Global challenges and prospects of photovoltaic materials disposal and recycling: A comprehensive review. Sustainability. 2022; https://doi.org/10.3390/su14148567
6. Guo J, Liu X, Yu J, Xu C, Wu Y, Pan D. An overview of the comprehensive utilization of silicon-based solid waste related to PV industry. Resour Conserv Recycl. 2021; https://doi.org/10.1016/j.resconrec.2021.105450
7. Majewski P, Al-shammari W, Dudley M, et al. Recycling of solar PV panels—product stewardship and regulatory approaches. Energy Policy. 2021; https://doi.org/10.1016/j.enpol.2020.112062

8. Wang X, Tian X, Chen X, Ren L, Geng C. A review of end-of-life crystalline silicon solar photovoltaic panel recycling technology. Sol Energy Mater Sol Cells. 2022; https://doi.org/10.1016/j.solmat.2022.111976
9. Kokul SR, Bhowmik S. Recycling of crystalline silicon photovoltaic solar panel waste to modified composite products. 2021; https://doi.org/10.1177/14777606211019416
10. Heath GA, Silverman TJ, Kempe M, et al. Research and development priorities for silicon photovoltaic module recycling to support a circular economy. Nat Energy. 2020; https://doi.org/10.1038/s41560-020-0645-2
11. Dias P, Schmidt L, Gomes LB, et al. Recycling waste crystalline silicon photovoltaic modules by electrostatic separation. J Sustain Metall. 2018; https://doi.org/10.1007/s40831-018-0173-5
12. Doni A, Dughiero F. Electrothermal heating process applied to c-Si PV recycling. IEEE Photovolt Spec Conf. 2012; https://doi.org/10.1109/PVSC.2012.6317715
13. Frisson L, Lieten K, Bruton T, et al. Recent improvements in industrial PV module recycling. Eur Photovolt Sol Energy Conf. 2020; 2160-2163.
14. Song B, Zhang M, Fan Y, et al. Recycling experimental investigation on end of life photovoltaic panels by application of high voltage fragmentation. Waste Manag. 2020; https://doi.org/10.1016/j.wasman.2019.10.015
15. Li X, Liu H, You J, et al. Back EVA recycling from c-Si photovoltaic module without damaging solar cell via laser irradiation followed by mechanical peeling. Waste Manag. 2022; https://doi.org/10.1016/j.wasman.2021.11.024
16. Azeumo MF, Germana C, Ippolito NM, et al. Photovoltaic module recycling, a physical and a chemical recovery process. Sol Energy Mater Sol Cells. 2019; https://doi.org/10.1016/j.solmat.2019.01.035
17. Pang S, Yan Y, Wang Z, et al. Enhanced separation of different layers in photovoltaic panel by microwave field. Sol Energy Mater Sol Cells. 2021; https://doi.org/10.1016/j.solmat.2021.111213
18. Granata G, Pagnanelli F, Moscardini E, et al. Recycling of photovoltaic panels by physical operations. Sol Energy Mater Sol Cells. 2014; https://doi.org/10.1016/j.solmat.2014.01.012
19. Wang T-Y, Hsiao J-C, Du C-H. Recycling of materials from silicon base solar cell module. IEEE Photovolt Spec Conf. 2012; 002355-002358.
20. Dias P, Javimczik S, Benevit M, Veit H. Recycling WEEE: Polymer characterization and pyrolysis study for waste of crystalline silicon photovoltaic modules. Waste Manag. 2017; 60:716-722.
21. Ismail H, Hanafiah MM. A review of sustainable e-waste generation and management: Present and future perspectives. J Environ Manage. 2020; https://doi.org/10.1016/j.jenvman.2020.110495
22. Izhevskyi VA, Genova LA, Bressiani JC, Bressiani AHA. Silicon carbide: Structure, properties and processing. Cerâmica. 2000; https://doi.org/10.1590/S0366-69132000000100002
23. Anjana EI, CS S, Akhil MG, et al. From solar waste panels. IEEE Trans Plasma Sci. 2024; https://doi.org/10.1109/TPS.2023.3325273
24. Pak YA, Bolatova Z, Nikitin DS, et al. Glass waste derived silicon carbide synthesis via direct current atmospheric arc plasma. Waste Manag. 2022; https://doi.org/10.1016/j.wasman.2022.04.002
25. Bolatova Z, Pak A, Larionov K, et al. Ash and slag waste processing in self-shielded atmospheric DC arc discharge plasma. Materials (Basel). 2022; https://doi.org/10.3390/ma15228134
26. Anjana EI, Akhil MG, Venkatesan J, Jayasankar K. Thermal plasma synthesis of silicon carbide from solar waste panels. IEEE Trans Plasma Sci. 2023; 52(7): 2602-2608.

27. Lee Y, Kwon O-K, Sun J-H, et al. Synthesis of silicon carbide powder using recovered silicon from solar waste silicon wafer. Resour Recycl. 2022; 31(5): 52-58.
28. Williams PT, Besler S. The influence of temperature and heating rate on the slow pyrolysis of biomass. Renew Energy. 1996; https://doi.org/10.1016/0960-1481(96)00006-7
29. Jahirul MI, Rasul MG, Chowdhury AA, Ashwath N. Biofuels production through biomass pyrolysis: A technological review. Energies. 2012; https://doi.org/10.3390/en5124952
30. Pak AY, Mamontov GY, Slyusarskiy KV, et al. Ash waste utilization via direct current arc plasma with production of SiC and AlN. Waste Biomass Valorization. 2021; 1-12.
31. Klemchuk P, Ezrin M, Lavigne G, et al. Investigation of the degradation and stabilization of EVA-based encapsulant in field-aged solar energy modules. Polym Degrad Stab. 1997; 55(3): 347-365.
32. Polanský R, Pinkerová M, Bartunková M, Prosr P. Mechanical behavior and thermal stability of EVA encapsulant material used in photovoltaic modules. J Electr Eng. 2013;64(6): 361.
33. Marín ML, Jiménez A, López J, Vilaplana J. Thermal degradation of ethylene (vinyl acetate): Kinetic analysis of thermogravimetric data. J Therm Anal Calorim. 1996; 47(1): 247-258.
34. Guizani C, Jeguirim M, Valin S, et al. Biomass chars: The effects of pyrolysis conditions on their morphology, structure, chemical properties and reactivity. Energies. 2017; https://doi.org/10.3390/en10060796
35. Larionov KB, Povalyaev PV, Bolatova ZS, et al. Plasma gasification of frying oil to produce hydrogen-rich synthesis gas and nanodispersed carbon material. Biomass Bioenergy. 2025; https://doi.org/10.1016/j.biombioe.2025.107645
36. Шевко ВМ, Сержанов ГМ, Бадикова АД, Утеева РА. Термоповедение силицидов железа. Междунар журнал прикл и фунд исслед. 2014; (10-3): 41-45.
37. Chiang PF, Han S, Claire MJ, et al. Sustainable treatment of spent photovoltaic solar panels using plasma pyrolysis technology and its economic significance. Clean Technol. 2024; https://doi.org/10.3390/cleantechnol6020022
38. Roy J, Chandra S, Das S, Maitra S. Oxidation behaviour of silicon carbide: A review. Rev Adv Mater Sci. 2014; 38(1):29-39.
39. Park DJ, Jung YI, Kim HG, et al. Oxidation behavior of silicon carbide at 1200°C in both air and water–vapor-rich environments. Corros Sci. 2014; https://doi.org/10.1016/j.corsci.2014.07.052
40. Ивенин СВ, Крестьянсков ФЮ. Быстрое термическое окисление карбида кремния. Огарёв-Online. 2014; 3 (17):1-7.
41. Phadatare M, Patil R, Blomquist N, et al. Silicon-nanographite aerogel-based anodes for high performance lithium ion batteries. Sci Rep. 2019; https://doi.org/10.1038/s41598-019-51087-y
42. Zhou C, Bai N, An B, Li J. Reusing waste photovoltaic solar cells: Preparation of SiC-AlN composite ceramic materials. Sol Energy Mater Sol Cells. 2025; https://doi.org/10.1016/j.solmat.2025.113443